In Vitro Cell.Dev.Biol.—Animal (2013) 49:785–797
DOI 10.1007/s11626-013-9666-5

Significant role of μ-calpain (CANP1) in proliferation/survival of bovine skeletal muscle satellite cells

Hoa Van Ba · Hwang Inho

Received: 1 March 2013 / Accepted: 8 July 2013 / Published online: 13 August 2013 / Editor: T. Okamoto

Abstract Calpains are a family of Ca^{2+}-dependent intracellular cysteine proteases, including the ubiquitously expressed μ-calpain (CANP1) and m-calpain (CANP2). The CANP1 has been found to play a central role in postmortem proteolysis and meat tenderization. However, the physiological roles of CANP1 in cattle skeletal satellite cells remain unclear. In this study, three small interference RNA sequences (siRNAs) targeting CANP1 gene were designed and ligated into pSilencer plasmid vector to construct shRNA expression constructs. Suppression of CANP1 in satellite cells was evaluated using these shRNA expressing constructs. Our results revealed that all three siRNAs could downregulate the expression of CANP1. Suppression of CANP1 significantly reduced cell viability in cell proliferation when compared with control cells. We found a crosstalk between CANP1 and caspase systems, particularly suppression of CANP1 resulted in an increase in the expressions of apoptotic caspases such as caspase-3, caspase-6, caspase-7, caspase-8, and caspase-9, as well as heat-shock protein (HSP) systems. Additionally, suppression of CANP1 led to the upregulation of other apoptosis and DNA damage-regulating genes whilst at the same time downregulating proliferation, migration, and differentiation-regulating genes. The results of our findings report for the first time that suppression of CANP1 resulted in the activation of caspase and HSP systems which might in turn regulate apoptosis through the caspase-dependent cell death pathway. This clearly demonstrates the key roles of CANP1 in regulation of cell proliferation and survival.

Keywords μ-Calpain · Caspases · Heat-shock protein · Knockdown · Satellite cell

Introduction

Calpains are a family of Ca^{2+}-dependent intracellular cysteine proteases, including the ubiquitously expressed μ-calpain (CANP1) and m-calpain (CANP2). Both CANP1 and CANP2 are heterodimers, consisting of a distinct large 80-kDa catalytic subunit, encoded by the genes CANP1 and CANP2. Several studies on meat muscle tissue have shown that the calpain proteolytic system plays a central role in postmortem proteolysis and tenderization (Huff-Lonergan and Lonergan 2005; Gandolfi et al. 2011). High calpain activity leads to the improvement of meat tenderness (Kent et al. 2004; Kemp et al. 2010). However, some studies (using either in vitro or in vivo models) demonstrated that, among the ubiquitous calpains, CANP1 has the most significant role in postmortem proteolysis and meat tenderization, whereas CANP2 and calpain-3 do not autolyze in postmortem muscle and are therefore not involved in postmortem tenderization (Koohmaraie et al. 1987; Geesink et al. 2006; Kemp et al. 2010).

The physiological function of calpains in living organisms such as cell lines and animals is still not fully understood, and a lot of controversies exist. Calpain activity is regulated by a variety of factors, including Ca^{2+}, phospholipids, endogenous calpain-specific inhibitor peptide, and calpastatin (Sorimachi et al. 1997; Goll et al. 2003). It has been reported that calpains are apparently involved in a multitude of physiological and pathological events. Previous studies using synthetic inhibitors have implicated the role of calpains in various pathological processes (Huang and Wang 2001) and physiological processes (depending on cell lines and species) such as cell spreading, cell migration and attachment, motility, myoblast fusion, and apoptosis (Huttenlocher et al. 1997; Potter et al. 1998; Goll et al. 2003; Dedieu et al. 2004; Honda et al. 2008).

Electronic supplementary material The online version of this article (doi:10.1007/s11626-013-9666-5) contains supplementary material, which is available to authorized users.

H. Van Ba · H. Inho (✉)
Department of Animal Science and Biotechnology, Chonbuk National University, Jeonju 561-756, Republic of Korea
e-mail: hoasaudau_85@yahoo.com

Since conventional inhibitors used for the studies of the functions of these enzymes lack specificity, the individual physiological function and biochemical mechanism of these three isoforms, especially CANP1, are not clear. In contrast, in recent years, RNA interference (RNAi) mediated by small interfering RNA (siRNA) has been widely used in gene function studies (Xia et al. 2002; Jain et al. 2010). The RNAi method usually utilizes short hairpin RNA (shRNA) expressed from plasmid vector. The shRNA expressing construct is integrated into the genome, becomes a sustainable source of siRNA, and produces sustained RNAi effects. Thus, the RNAi strategy, which can inhibit each calpain isoforms specifically, would be a powerful tool to clarify physiological functions. Although a number of studies found that CANP1 has a central role in muscle proteolysis and meat tenderization processes, and it also plays some physiological roles in some cell lines as mentioned above. However, the exact role of CANP1 in cellular processes of bovine skeletal satellite cells remained unknown till now. Since cattle are important animals with significant economic value. Understanding the role of particular genes which regulate the growth and myogenesis process are extremely important to control the muscle tissue growth in particular. Herein, we used siRNAs to generate a specific knockdown of CANP1 at the cellular level. We generated CANP1 knockdown of the satellite cells isolated from Korean native cattle, using pSilencer plasmid vector-mediated siRNAs and provided clear evidence that CANP1 is mainly involved in proliferation and survival of bovine skeletal satellite cells.

Materials and Methods

Cell preparation and culture. The satellite cells were isolated from 24-mo-old Korean native cattle (Hanwoo) following the method of Dodson et al. (1987). The entire work involving the use of animals was approved by an Institutional Animal Care and Use Committee. Briefly, the semitendinosus muscle (500 g) was excised from Korean native cattle immediately after slaughter at a commercial abattoir (located in Jeonju province, South Korea). The connective tissue and most of the fat were trimmed off and discarded. The muscle was cut into small fragments (about 3 mm^3). After enzymatic digestion with 1% pronase solution (Sigma, St. Louis, MO) at 37°C for 60 min, single cells were separated from the fragments by repeated centrifugation at 1,000×*g* for 10 min at room temperature. The primary muscle cells were cultured in Dulbecco's modified Eagle's medium (DMEM) (Gibco, Grand Island, New York) supplemented with 15% fetal bovine serum (Gibco), 100 IU/ml penicillin, and 100 μg/ml streptomycin (Sigma) in a humidified incubator at 37°C with 5% CO_2. To isolate satellite cells from the primary muscle cells, the cells were applied to a magnetic cell sorting system (AutoMACS, Milteny Biotech, Bergisch Gladbach, Germany); when the cells reached 80% confluence, they were collected and re-suspended in 1× phosphate-buffered saline (PBS, Gibco) supplemented with 0.5% bovine serum albumin and 2 mM EDTA. After centrifugation (1,500×*g* for 5 min), the cell pellet was re-suspended in 1× PBS (100 μl) containing 10 μg anti-M-cadherin antibodies (DB BioScience, San Diego, CA) and then incubated with 20 μl of anti-mouse IgG1 micro beads at 4°C for 30 min. Finally, cell suspension (10^7 cells in 2 ml PBS) was loaded into a magnetic cell sorting system to isolate satellite cells. After sorting, the positive cells were counted using a hemacytometer, and the percentage of satellite cells was determined. Furthermore, to confirm whether the isolated cells are really myogenic satellite cells, the positive cells were also cultured in myogenic differentiation medium (DMEM containing 2% horse serum) for 7 d to check the myotube formation. The cells were stained with hematoxylin solution (Sigma) and finally stained with eosin solution (Muto Pure Chemicals Co, Tokyo Japan).

Designing of siRNA and construction of plasmid vector. Three siRNA sequences against CANP1 were designed as per the siRNA designing program (http://www.ambion.com/techlib/misc/siRNA_design.html). The siRNAs were converted to shRNAs by using the siRNA target finder program for the pSilencer vector on the web page (http://www.ambion.com/techlib/misc/psilencer_converter.html). The three target sequences for constructing pSilencer plasmid vector against CANP1 were named as CANP1-siRNA1 top: (5′-GAT CCG CTG GAACACCACCCTGTATTTCAA GAGAATA CAGGGTGGTGTTCCAGTTTTTTGGAAA-3′) and CANP1-siRNA1 bottom: (5′-AGCTTTTCCAAAAAACT GGAACACCACCCTGTATTCTCTTGAAATACAGGGT-GGTGTTCCAGGG-3′); CANP1-siRNA2 top: (5′-GAT CCGCTTCAAGTCCCTCTTCAGATTCAA GAGATCT GAAGAGGGACTTGAAGTTTTTTGGAAA-3′) and CANP1-siRNA2 bottom: (5′-AGCTTTTCCAAAAAA CTTCAAGTCCCTCTTCAGATCTCTTGAATCTGAAGA-GGGACTTGAAGCG-3′); CANP1-siRNA3 top: (5′-GATCCGCAAGGAAGGTGACTTTGTGTTCAA GAGACACAAAGTCACCTTCCTTGTTTTTTGGAAA-3′) , and CANP1-siRNA3 bottom: (5′-AGCTTTTCCAAAAAA CAAGGAAGGTGACTTTGTGTCTCTTGAACACAAAG-TCACCTT CCTTGCG-3′). These oligo sequences were annealed, and the resulting annealed shRNAs were ligated into pSilencer hygro vectors by T4 DNA ligase between the BamH I and Hind III restriction sites according to the manufacturer's instructions. The ligated product (shRNA expression constructs) was transformed into *Escherichia coli* GC^{TM} competent cells (Sigma) following the manufacturer's protocol. After amplification, the ligated product was isolated using a GenElute Plasmid Miniprep Kit (Sigma) and then was digested by endonuclease BamH I and Hind III restriction enzymes. The digested product (shRNA and plasmid vectors)

was visualized by agarose gel electrophoresis and then used for the transfection.

Transfection of shRNA expression constructs. The isolated satellite cells were grown in DMEM in a humidified incubator at 37°C with 5% CO_2. Cells were transfected with either shRNA expression constructs or pSilencer hygro vector negative control (control) using Lipofectamine 2000™ reagent (Invitrogen, Carslbad, CA) according to the manufacturer's instructions. Following the transfection, the cells were incubated for 24 h and then were used to investigate the transfection efficiency, confocal scanning laser microscope (CSLM), and microarray analysis.

Cell viability assay. Cell viability was determined by using CCK-8 colorimetric assay. Briefly, cells were seeded into 96-well plates with 100 μl growth medium without antibiotics at density of 2×10^4 cells/well. One day after, the cells were transfected with either 100 ng of shRNA expression constructs or pSilencer hygro vector negative control as described above in the present study. Twenty-four hours after transfection, 10 μl of CCK-8 solution was added to each well and incubated for 4 h at 37°C in a humidified incubator. The light absorption was measured at 450 nm with a microplate reader (Bio-Rad, Hercules, CA). The cell viability was expressed as a percent of control culture value.

Confocal scanning laser microscope. (CSLM) The cells were transfected with either CANP1-siRNA expression constructs or pSilencer hygro vector negative control as described above in the present study. The transfected cells were then stained with contents of live/dead cytotoxicity kit following the previously established method (Amna et al. 2013). Finally, the stained cells were observed under the fluorescence microscope.

Real-time polymerase chain reaction. To assay the efficiency of CANP1 suppression by siRNA transfections and the possibility the siRNAs-induced cell death is regulated by particular genes, the analyses of CANP1, caspase-3 (CASP3), caspase-7 (CASP7), caspase-9 (CASP9), heat-shock protein 27 (HSP27), heat-shock protein 70 (HSP70), and heat-shock protein 90 (HSP90) mRNA expression in the shRNA expression constructs-transfected cells and control cells were carried out using real-time polymerase chain reaction (RT-PCR) (CFX96™ Real-Time PCR Detection Systems, Bio-Rad). Twenty-four hours after transfection, total RNA was extracted from the satellite cells using a RNA isolation kit, TRIzol (Sigma-Aldrich). cDNA was synthesized from the total RNA using the reverse transcriptase first-strand cDNA synthesis kit according to the manufacturer's protocols. Primers specific for the *Bos taurus* CANP1, CASP3, CASP7, CASP9, HSP27, HSP70, HSP90, and a housekeeping gene glyceraldehyde 3-phosphate dehydrogenase (GAPDH) used in this research were as follows: CANP1 (forward 5′-CCCTCAATGACA CCCTCC-3′ and reverse 5′-TCCACCCACTCACCAAACT-3′); CASP3 (forward 5′-GTTCATCCAGGCTCTTTG-3′ and reverse 5′-TCTATTGCTACCTTTCG-3′); CASP7 (forward 5′-GAATGGGTGTCCGCAACG-3′ and reverse 5′-TTGG CACAAGAGCAGTCGTT-3′); CASP9 (forward 5′-CGC CACCATCTTCTCCCTG-3′ and reverse 5′-CCAACGTCT CCTTCTCCTCC-3′); HSP27 (forward 5′-ACCA TTCCCGTCACCTTCC-3′ and reverse 5′-TCTTTA CTTGTTTCCGGCTGTT-3′); HSP70 (forward 5′-CGTG ATGACCGCCCTGAT-3′ and reverse 5′-CGGCTGG TTGTCCGAGTA-3′); HSP90 (forward 5′-TTGGCTATCC CATCACTC-3′ and reverse 5′-TTCTATCTCGGGCTTGTC-3′); and a housekeeping gene GAPDH (forward 5′-CACC CTCAAGATTGTCAGC-3′ and reverse 5′-TAAGTCC CTCCACGATGC-3′). PCR was performed using 20 μl reaction volumes, containing 10 μl SsoFast™ EvaGreen® Supermix (Bio-Rad), 0.5 μl each (10 pmol/μl) of forward and reverse primers, 1 μl of cDNA (100 ng/μl), and 8 μl of nuclease-free water. The PCR thermal cycle reaction consisted of initial annealing at 57°C for 2 min, denature at 95°C for 3 min, followed by 40 cycles of denaturation and annealing at 95°C/10 s and 60°C/10 s, respectively. The relative expression of transcripts present for the measured genes in the satellite cells was normalized to GAPDH transcripts. Relative ratios were calculated using the method as discribed by Pfaffl (2001).

Preparation of cell lysates and Western blot. After 24 h of transfection, the transfected cells were harvested, and protein content was extracted using CelLytic™M kit (Sigma) according to the manufacturer's instructions. The protein concentration was determined using Bio-Rad protein assay kit (Bio-Rad). Whole protein (50 μg) of each sample was separated on 12.5% acrylamide with 4% acrylamide stacking gels. The proteins from gels were transferred to Hybond-P PVDF membrane (GE Healthcare, Amersham, UK) for 60 min at 200 mA. Membranes were blocked in 20 ml of blocking solution (20 mM Tris–HCl, 137 mM NaCl, 5 mM KCl, and 0.05% Tween 20) for 60 min and then incubated for 60 min at room temperature with either CANP1 (1:1,000), CASP9 (1:1,000), HSP27 (1:1,000), HSP90 (1:1,000), or actin (1:1,000) primary antibodies in blocking solution. Subsequently, the bound primary antibodies were then labeled with alkaline phosphate-conjugated rabbit anti-mouse IgG secondary antibody in blocking solution for 60 min at room temperature. The bound protein-antibodies were visualized by incubating the membrane with alkaline phosphate–conjugate substrate (Bio-Rad).

Microarray analysis. The total RNA was extracted from the transfected cells for microarray analysis. The synthesis of target cRNA probes and hybridization were performed using Agilent's LowInput QuickAmp Labeling Kit (Agilent Technology, Santa

Clara, CA) according to the manufacturer's instructions. The fragmented cRNA was then re-suspended with 2× hybridization buffer and directly pipetted onto assembled bovine (V2) gene expression 4×44K microarray (Agilent Technologies). The hybridization images were analyzed by Agilent DNA microarray Scanner (Agilent Technology), and the data quantification was performed using Agilent Feature Extraction software 10.7 (Agilent Technology). All data normalization and selection (fold-changed) were performed using GeneSpringGX 7.3.1 (Agilent Technology). Reliable genes were filtered by flag, following the Agilent manual. The average of normalized ratio was calculated by dividing the average of control normalized signal intensity by the average of test normalized signal intensity. Functional categorization of gene families over-represented was performed using the program from the NIAID web site (http://david.abcc.ncifcrf.gov/summary.jsp).

Statistic analysis. The experiments were performed in triplicates. ANOVA test was applied to test the significance of difference in the cell proliferation, mRNA, and protein expression levels between the cells transfected by three different shRNA expression constructs with pSilencer hygro vector negative control (control). All mean values were compared using the Duncan's multiple-range test at the 5% level of significance (SAS Institute, Cary, NC, 2007).

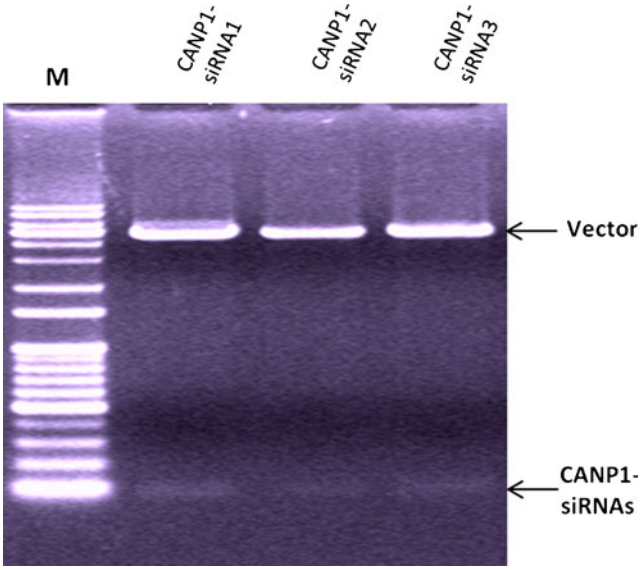

Figure 1. Agarose gel electrophoresis (1.8%) of colony plasmid DNA and CANP1-siRNAs digested with BamH I and Hind III. *M*: 100 bp DNA molecular weight marker; 4,885 bp of plasmid vector; 65 bp of CANP1-siRNA1, CANP1-siRNA2, and CANP1-siRNA3 oligonucleotides.

Results

Confirmation of shRNA constructs for RNAi study. The shRNA consists of a sense strand, a short loop sequence, an antisense strand, and following four continuous thymines RNA polymerase III terminator. All of the three annealed shRNA template inserts were ligated between the BamH I and Hind III sites of the pSilencer plasmid vector. Sixteen hours after the transformation of the constructs into the *E. coli* GC^{TM} competent cells, transformed cells produced distinct colonies on LB-agar plate containing ampicillin (50 μg/ml) as selective media. The expected CANP1-siRNAs and plasmid vector digested with BamH I and Hind III was visualized in 1.8% agarose gel electrophoresis (Fig. 1).

Transfection efficiency. In order to get effective siRNA sequences, three shRNA expression constructs were constructed. In this study, we optimized the transfection conditions, and the CANP1 mRNA as well as protein expression levels were assayed by RT-PCR and Western blot, respectively. Transfection with a plasmid encoding CANP1-siRNAs resulted in significant downregulation of mRNA and protein levels in satellite cells (Fig. 2). In particular, the relative mRNA expression levels of CANP1 gene in the cells transfected by CANP1-siRNA1, CANP1-siRNA2, and CANP1-siRNA3 constructs were reduced by 16.49%, 72.64%, and 85.54%, respectively, when compared with the control cells (Fig. 2*A*). Also, the protein level in CANP1-siRNA transfection was significantly lower than that observed in control cells (Fig. 2*B* and *C*).

Identification of satellite cells, cell viability, and CSLM assay. After sorting, the positive cells were counted, and the percentage of satellite cells was determined to be 12.5%. The percentage of fused cells (multinucleated myoplasts) was 25±1.5% at day 5 and increased to 30±2.3% at day 7 of incubation. The positive cells cultured in growth medium and finally cells from fourth passage were used for the cell viability and CSLM assay. Three separate shRNA expression constructs including CANP1-siRNA1, CANP1-siRNA2, and CANP1-siRNA3 were screened for their ability to silence CANP1gene expression in satellite cells. Following optimizing the transfection conditions for cell number, volume of transfection agent used, and the appropriate concentration of each shRNA expression constructs, the CCK-8 assay was used to assay the effect of CANP1 knockdown on cell viability in cell proliferation. Figure 3*A* shows the CCK-8 data of three different shRNA expression constructs at 24 h post-transfection. The obtained data clearly showed that all three CANP1-siRNAs significantly reduced the cell viability. The cell viability after 24 h transfection was reduced by 42.50%, 48.69%, and 63.20% in CANP1-siRNA1, CANP1-siRNA2, and CANP1-siRNA3, respectively, compared with the control cells. The present results indicate that the effect of CANP1 knockdown on the viable cells in cell proliferation varied depending on each CANP1-siRNA sequences. Additionally,

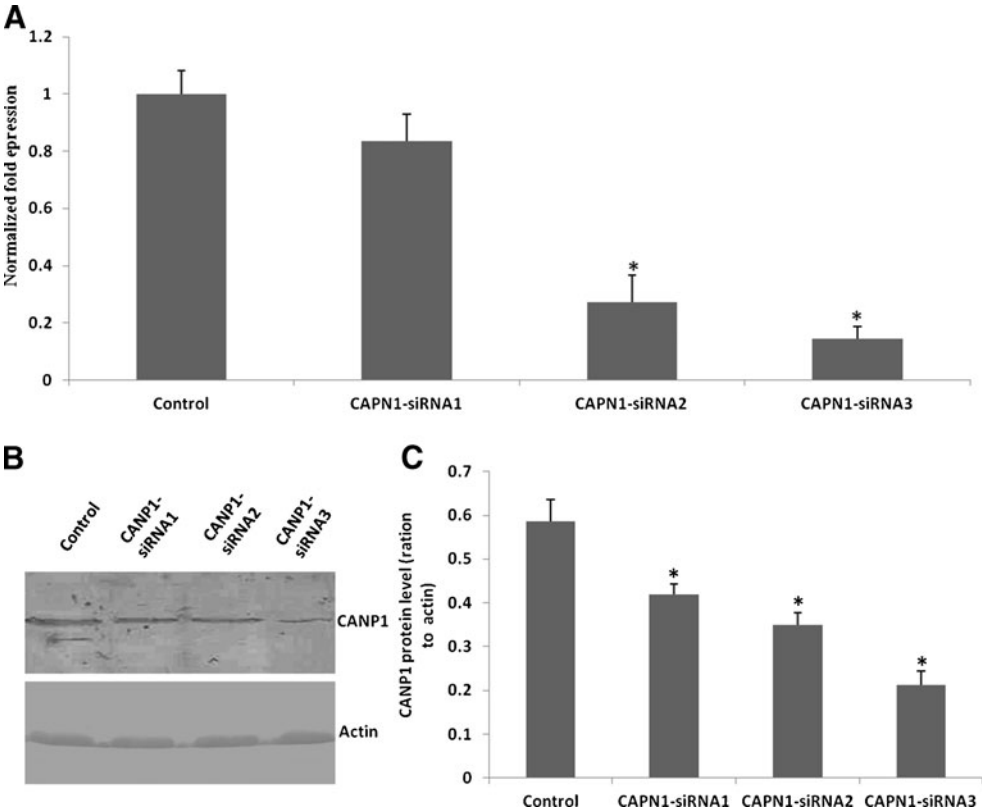

Figure 2. Knocking down of CANP1 in satellite cells analyzed at mRNA level and protein level. The mRNA and protein expression were assayed by RT-PCR and Western blot respectively following 24 h transfection. (*A*) RT-PCR with specific primers confirmed that CANP1 was silenced at the mRNA level. Value expressed as mean±standard error of mean (SEM), calculated from three independent experiments. Gene expression was normalized to GAPDH expression and denoted as a gene/GAPDH ratio. *$p<0.05$; (*B*) Showed Western blot graph; (*C*) showed relative densitometric values of Western blots. Western blot with anti-actin antibody was used as loading control.

no floating cells were observed in the control (Fig. 3*B*), whereas a large number of floating cells were seen after the CANP1-siNRAs transfection (Fig. 3*C*). Furthermore, the morphological changes and cell death by CANP1 knockdown was studied using confocal microscopy. The CSLM provides information about cell behavior in a wet environment. In the present study, because the CANP1-siRNA3 reduced the cell viability the most, we therefore selected the CANP1-siRNA3-transfected cells for the CSLM analysis. One can observe that no dead cells were found in the cells transfected with pSilencer hygro vector negative control (control) (Fig. 3*D*). However, dead cells were observed after 24 h CANP1-siRNA3 transfection (Fig. 3*E*). From the obtained CLSM images, it is clear that knockdown of CANP1 by specific CANP1-siRNAs caused cell death. The CLSM results are in good agreement with cell viability results by CCK-8 assay (Fig. 3*A*).

Gene expression profile. In order to understand the probable mechanism of cell death (apoptosis) caused by CANP1 suppression, we further studied the expressions of representative related genes as well as the genome of the transfected cells. In particular, we explored the mRNA expression of several representative apoptotic caspases and HSPs including CASP3, CASP7, CASP9 and HSP27, HSP70, and HSP90 by using RT-PCR technique. Our results pointed out that the CASP3 gene expression increased 1.49-, 1.67-, and 1.71-fold in the CAPN1-siRNA1, CAPN1-siRNA2, and CAPN1-siRNA3-transfected cells, respectively (Fig. 4*A*) when compared with control. The CASP7 gene expression increased 1.19-, 1.45-, and 1.58-fold in the CAPN1-siRNA1, CAPN1-siRNA2, and CAPN1-siRNA3-transfected cells, respectively (Fig. 4*A*). The CASP9 gene expression also increased 1.62-, 1.87-, and 2.39-fold in the CAPN1-siRNA1, CAPN1-siRNA2, and CAPN1-siRNA3-transfected cells, respectively (Fig. 4*A*). Similarly, the HSP27 gene expression increased 3.75-, 1.90-, and 3.22-fold relative to control cells in the CAPN1-siRNA1, CAPN1-siRNA2, and CAPN1-siRNA3-transfected cells, respectively (Fig. 4*B*). The HSP70 gene expression increased 1.13-, 1.52-, and 3.27-fold relative to control cells in the CAPN1-siRNA1, CAPN1-siRNA2, and CAPN1-siRNA3-transfected cells, respectively (Fig. 4*B*). The HSP90 gene expression also increased 4.14-, 2.25-, and 3.05-fold relative to control cells in the CAPN1-siRNA1, CAPN1-siRNA2, and CAPN1-siRNA3-transfected cells, respectively (Fig. 4*B*). Furthermore, we explored the protein expression levels of the representative CASP9, HSP27, and HSP90 genes by Western blot. The results showed that the CASP9, HSP27, and HSP90 protein levels in CAPN1-siRNAs transfected cells significantly increased (Fig. 5).

Even though RT-PCR with specific primers confirmed that CANP1 was silenced at the mRNA level, and CASP3, CASP7, CASP9, HSP27, HSP70, and HSP70 genes were upregulated in RT-PCR analysis, we were interested to double-check the expression level of these genes as well as the genome by using microarray analysis. The microarray

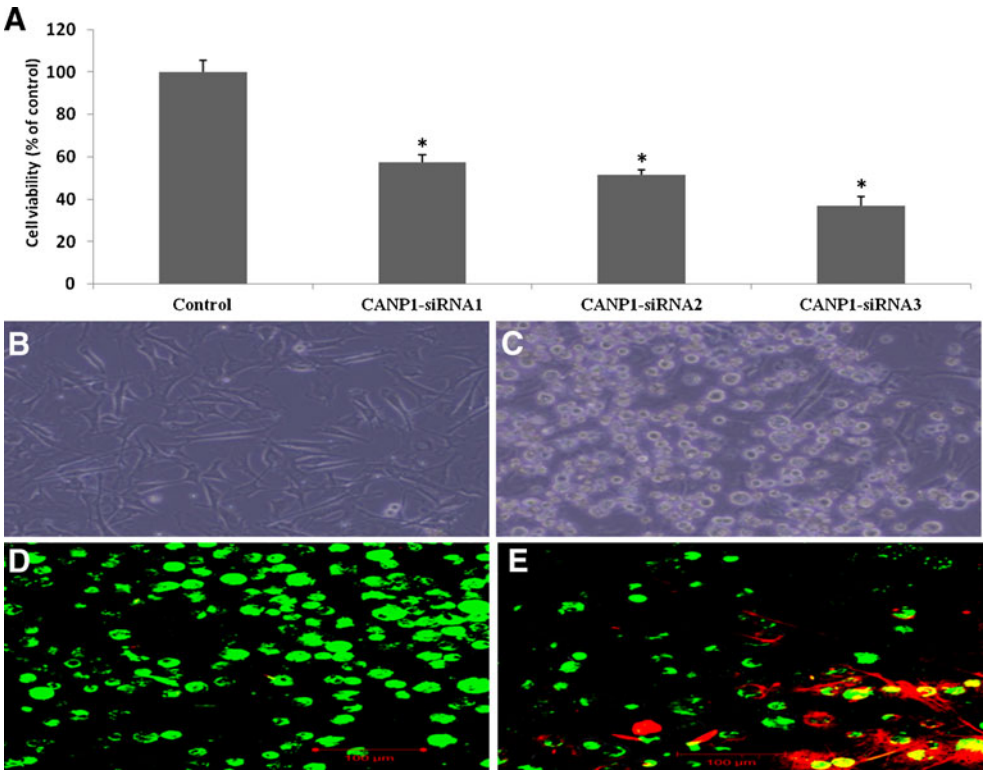

Figure 3. Effect of CANP1 suppression on satellite cell viability in cell proliferation. (*A*) The proliferation of cells following transfections as indicated was assayed by the CCK-8 assay. Data represent the mean±standard error of mean (SEM) of triplicates, *$p<0.05$. Representative images of transfected cells which were taken by electronic microscope at ×40 magnification, (*B*) represents the control cells; (*C*) represents the CANP1-siRNA3-transfected cells; (*D*) represents the confocal scanning laser microscope (CSLM) image of control cells; (*E*) represents the CSLM image of CANP1-siRNA3-transfected cells. The cells were stained by DiOC18 (3)/PI. Dead cells are labeled by PI and have red nuclei. Live cells are labeled by DiOC18 (3) and have green nuclei.

technique provides information about genetic regulatory pattern changes of large numbers of genes induced by various stimuli. As indicated by the present results, the CANP1-siRNA3 reduced the cell viability the most. It also showed the highest silencing capacity; therefore, we chose the CANP1-siRNA3-transfected cells for the microarray analysis. Similarly, the results of microarray analysis showed that CAPN1 expression was reduced significantly whereas CASP3, CASP7, CASP9, HSP27, HSP70, and HSP90 mRNA expressions were increased significantly (Fig. 6). The results of microarray analysis were consistent with the results obtained in the RT-PCR (Fig. 6).

In addition to the aforementioned genes, we also analyzed expression profiling of genomes of the cells following the transfections. Interestingly, we observed that 12,809 genes were upregulated, whereas 14,418 genes were downregulated. On the other hand, we compared the gene expression profiles in CAPN1-siRNA3-transfected cells and control cells. In the

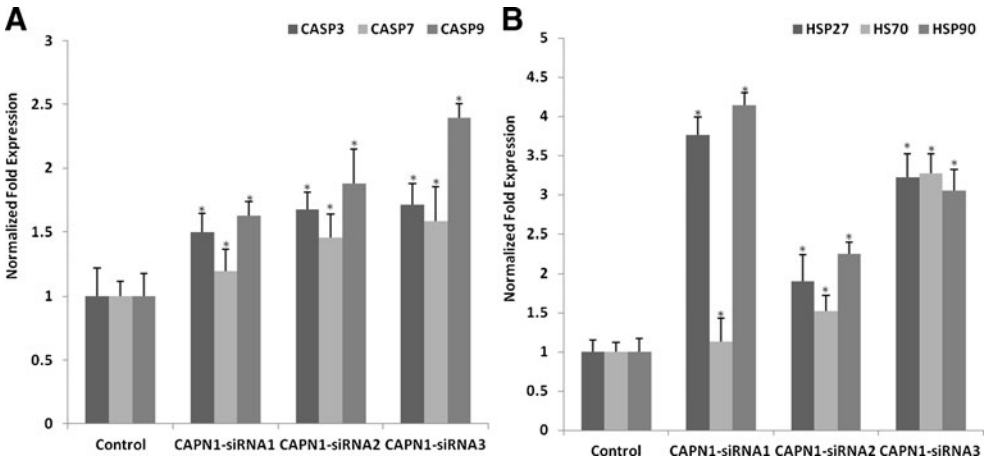

Figure 4. CASP3, CASP7, CASP9, HSP27, HSP70, and HSP90 mRNA expression levels in satellite cells. The mRNA expressions of these genes were assayed by quantitative real-time PCR following 24 h transfection with shRNA expression constructs or control. (*A*) Showed the quantitative RT-PCR results of caspase-3, caspase-7, and caspase-9; (*B*) Showed the quantitative RT-PCR results of HSP27, HSP70, and HSP90. Values expressed as mean±standard error of mean (SEM), calculated from three independent experiments. Gene expression was normalized to GAPDH expression and denoted as a gene/GAPDH ratio, *$p<0.05$.

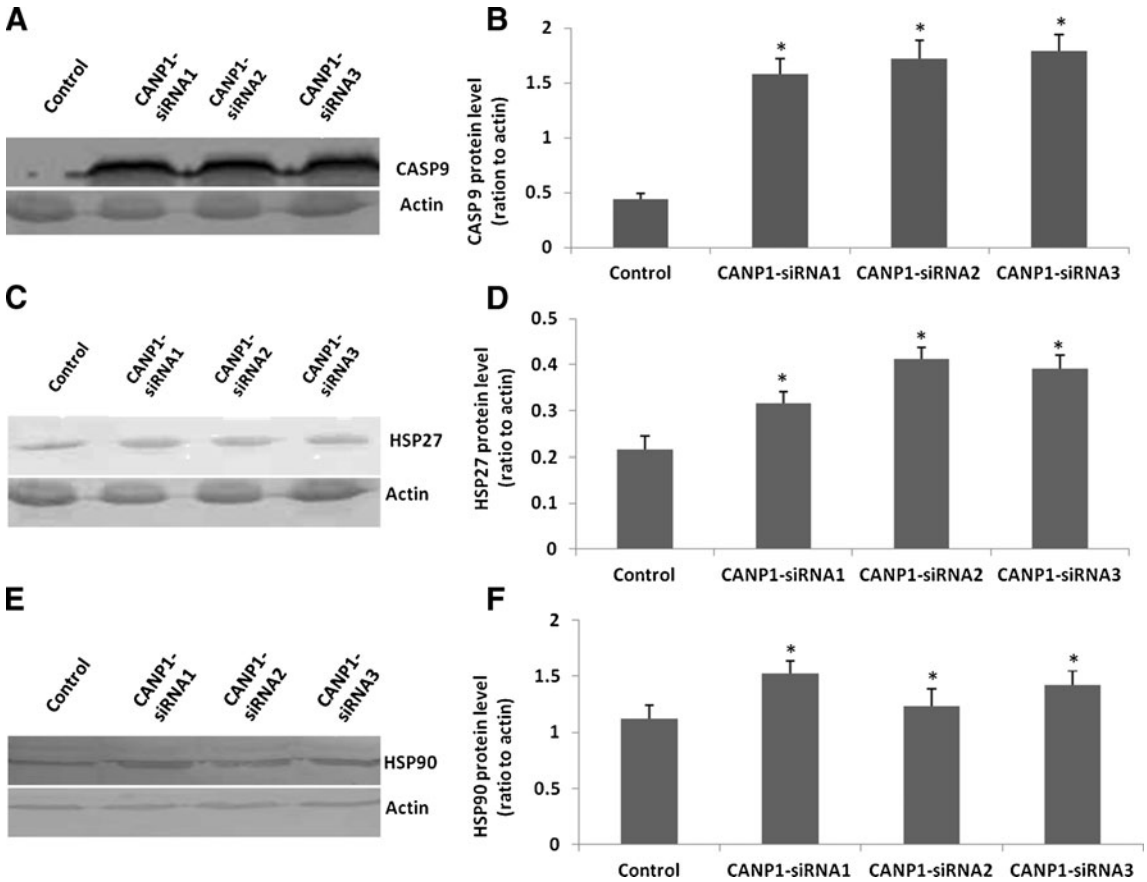

Figure 5. Knocking down of CANP1 in satellite cells analyzed at protein level of representative genes. Cells were transfected with CANP1-siRNA1, CANP1-siRNA2, and CANP1-siRNA3 expression constructs or control for 24 h. (*A*) showed Western blot graph of CASP9; (*B*) showed relative densitometric values of CASP9 Western blot. (*C*) Showed Western blot graph of HSP27; (*D*) showed relative densitometric values of HSP29 Western blot. (*E*) Showed Western blot graph of HSP90; (*F*) showed relative densitometric values of HSP90 Western blot. Western blot with anti-actin antibody was used as loading control.

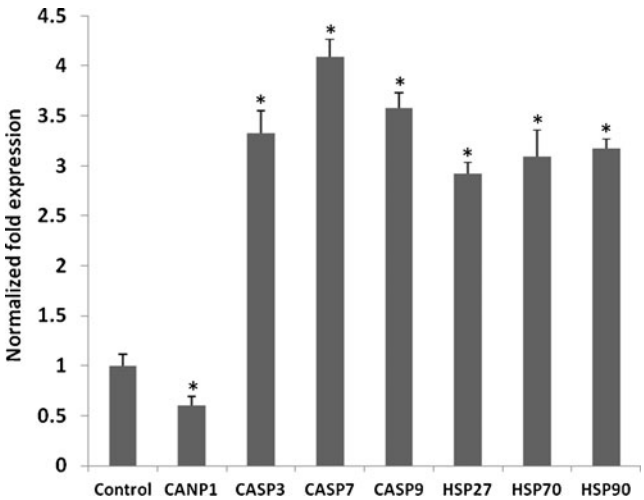

Figure 6. Microarray analysis of CANP1, CASP3, CASP7, CASP9, HSP27, HSP70, and HSP90 gene expressions in satellite cells which were transfected with the representative CANP1-siRNA3 for 24 h. The expression level of transfected cells was calculated based on the respective control values.

scatter plot shown in Fig. 7, the position of each gene on the plot is determined by its expression level in both CAPN1-siRNA3-transfected cells (*x*-axis) and control cells (*y*-axis). Genes with identical or similar expression are depicted by a black line whereas the gene clusters around the red line depicts the ≥2-fold upregulation. The green solid line demonstrates the ≤2-fold downregulation. The red spots at the top of red line indicate ≥3-fold upregulation whereas the blue spots at the bottom of green line illustrate ≤3-fold downregulation, respectively. We identified 437 genes (1.25% of 34,726 genes examined) whose expression level in CAPN1-siRNA3-transfected cells was ≥2-fold higher than those of control cells, and 150 genes (0.43% of 34,726 genes examined) expression level was ≤2-fold lower than those in control cells.

By comparing CAPN1-siRNA3-transfected cells with control cells, we identified 50 genes that were downregulated at least ≤3-fold after transfected by CAPN1-siRNA3. The downregulated genes were grouped according to the biologically functional categories, including regulation of cell proliferation (18 genes), muscle cell differentiation (9 genes), positive regulation of

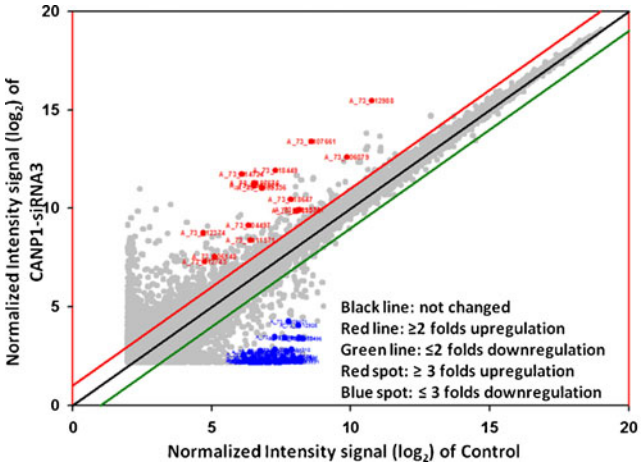

Figure 7. Expression profiling of genes in CANP1-siRNA3-transfected cells and control cells. The gene expression profiles of transfected cells or control were assessed using microarray analysis. Genes present on the bovine gene expression microarray were plotted using a scatter plot. The position of each gene on the plot is determined by its expression levels in control (*x*-axis) and CANP1-siRNA-transfected cells (*y*-axis).

multicellular organismal process (11 genes), and cell migration (12 genes) (Table 1). On the other hand, we identified 64 genes that were significantly upregulated by at least ≥3-fold following 24 h CAPN1-siRNA3 transfection. The upregulated genes were also grouped according to the biologically functional categories, including defense stress/response (13 genes), regulation of apoptosis or cell death program (49 genes), and response to DNA damage stimuli (2 genes) (Table 2).

Discussion

In this study, the primary satellite cells were derived directly from semitendinosus muscle of 24-mo-old Korean native cattle. The in vitro properties exhibited by primary cultures of satellite cells more closely reflect their in vivo properties than those exhibited by transformed cell lines (Allen 1987). Numerous studies have been carried out in which animals were chosen as key experimental units to develop species-specific satellite cell cultures (Greenlee et al. 1995; Burton et al. 2000). However, all of these satellite cell researchers worry about contaminating cells such as fibroblasts, which get co-isolated with satellite cells during cell isolation regimens. These contaminating cells potentially could overrun the cultures and provide biased measures of cell activity in vitro (Rhoads et al. 2009). However, in the present study, to decrease the presence of non-myogenic cells in primary cultures, the cell suspensions were loaded onto a magnetic cell sorting system, to isolate the satellite cells and ensure that culture systems were control and interpretable. Addtitionally, after the cell sorting to confirm whether the positve cells are really satellite cells, we

Table 1. A total of 50 genes is significantly ≤3-fold downregulated following 24 h CANP1-siRNA3 transfection

Functional category	Gene ID	Gene name	Species
Regulation of cell proliferation	NM_001076804	GATA binding protein 3	*Bos taurus*
	NM_001076198	RAS-like, estrogen-regulated, growth inhibitor	*B. taurus*
	NM_001105340	TNF receptor-associated factor 5	*B. taurus*
	NM_001075986	Adenomatous polyposis coli	*B. taurus*
	NM_173888	Adrenomedullin	*B. taurus*
	NM_174501	Arachidonate 15-lipoxygenase	*B. taurus*
	NM_181010	Endothelin 1	*B. taurus*
	NM_001083689	Forkhead box P1	*B. taurus*
	NM_001035463	Glypican 3	*B. taurus*
	NM_001105424	Hematopoietically expressed homeobox	*B. taurus*
	NM_001102175	Interleukin 20 receptor beta	*B. taurus*
	NM_001098385	Keratin 4	*B. taurus*
	NM_001076104	Nuclear factor I/B	*B. taurus*
	NM_001167900	Nuclear receptor subfamily 2, group E, member 3	*B. taurus*
	NM_001040645	Paired box 6	*B. taurus*
	NM_181024	Peroxisome proliferator-activated receptor gamma	*B. taurus*
	XM_613125	Phosphatase and tensin homolog	*B. taurus*
	NM_174196	Thrombospondin 1	*B. taurus*
Muscle cell differentiation	XM_001253596	GATA-6	*B. taurus*
	NM_001015600	Cytokeratin 19	*B. taurus*
	NM_001081515	Dual-specificity tyrosine	*B. taurus*
	NM_001083689	Forkhead box P1	*B. taurus*

Table 1. (continued)

Functional category	Gene ID	Gene name	Species
	NM_001077843	Low-density lipoprotein receptor-related protein 4	*B. taurus*
	NM_001040478	Myogenic differentiation 1	*B. taurus*
	NM_001077988	Neurotrophin 3	*B. taurus*
	NM_173951	Plasminogen	*B. taurus*
	NM_001076907	Retinoblastoma1	*B. taurus*
Positive regulation of multicellular organismal process	NM_174537	Fc fragment of IgE, high affinity I	*B. taurus*
	NM_001076804	GATA binding protein 3	*B. taurus*
	NM_001077111	Caspase recruitment domain family, member 9	*B. taurus*
	NM_174270	Cholinergic receptor, muscarinic 3	*B. taurus*
	NM_173877	Coagulation factor II (thrombin)	*B. taurus*
	NM_181010	Endothelin 1	*B. taurus*
	NM_001166609	Heat-shock 60 kDa protein 1 (chaperonin)	*B. taurus*
	NM_001102175	Interleukin 20 receptor beta	*B. taurus*
	NM_001038674	Lipopolysaccharide binding protein	*B. taurus*
	NM_173951	Plasminogen	*B. taurus*
	NM_174196	Thrombospondin 1	*B. taurus*
Cell migration	NM_175796	ATP synthase, mitochondrial F1 complex	*B. taurus*
	NM_174009	CD34 molecule	*B. taurus*
	NM_174537	Fc fragment of IgE, receptor for gamma	*B. taurus*
	NM_001101171	Abl interactor 2	*B. taurus*
	NM_001075986	Adenomatous polyposis coli	*B. taurus*
	NM_001113174	Chemokine (C–X–C motif) ligand 12	*B. taurus*
	NM_001075845	Empty spiracles homeobox 2	*B. taurus*
	NM_001110000	Kinase insert domain receptor	*B. taurus*
	NM_181037	Nitric oxide synthase 3 (endothelial cell)	*B. taurus*
	NM_175804	Nuclear receptor subfamily 2, group F, member 1	*B. taurus*
	NM_001034387	Nucleoporin 85 kDa	*B. taurus*
	NM_174435	Protein kinase C, alpha	*B. taurus*

also cultivated the positve cells in the myogenic differentiation medium (DMEM containing 2% horse serum) for 7 d and confirmed the capacity of myotube formation of the cells. Thus, from our screening experiment, it is concluded that the isolated cells have a potential of myogenesis differentiation into myotubes; therefore, we confirmed that the isolated cells are really myogenic satellite cells.

In this study, three siRNA sequences silencing CANP1 mRNA in cattle skeletal satellite cells with the highest scores were selected on the basis of ranking criteria of Reynolds et al. (2004). Several workers have also reported the efficient silencing of specific genes by RNAi approach using plasmid vectors to transfect into the fibroblast cells (Golding et al. 2006). In the present experiment, suppression of CANP1 by the all three shRNA expression constructs resulted in a significant reduction of viable cells in cell proliferation. Furthermore, the cell behavior was also tested by CLSM analysis; the CLSM images clearly demonstrated that knockdown of CANP1 by specific CANP1-siRNA3 resulted in the cell death whereas normal growth was observed in control cells. The results of the cell viability assay and CLSM analysis clearly indicated a crucial role of CANP1 in cell proliferation as well as survival of bovine satellite cells. On the other hand, a recent study (Azam et al. 2001) using in vivo model has demonstrated that inactivation of CANP1 in mice resulted in platelet dysfunction. However, the mutant mice displayed normal growth suggesting that the physiological function of CANP1 may be different depending on the cell types and animal species. Huttenlocher et al. (1997) also found that inhibition of CANP1 in Chinese hamster ovary cell lines resulted in inhibition of cell migration. In our study, it was also found that knockdown of CANP1 led to the downregulation of the migration-regulating genes. Moreover, the knockdown of CANP1 also resulted in a downregulation of proliferation-regulating genes (Table 1), indicating that CANP1 not only plays an important role in the regulation proliferation but also the migration of the skeletal muscle satellite cells. More recently, Dedieu et al. (2004) reported that inhibition of both

Table 2. Totals of 64 genes are significantly ≥3-fold upregulated following 24 h CANP1-siRNA3 transfection

Functional category	Gene ID	Gene name	Species
Defense/stress response	NM_001034735	CD74 molecule, major histocompatibility complex	*B. taurus*
	NM_001076918	Toll-like receptor 10	*B. taurus*
	NM_174263	Chemokine (C–C motif) ligand 20	*B. taurus*
	NM_175827	Chemokine (C–C motif) ligand 5	*B. taurus*
	NM_174299	Chemokine (C–X–C motif) ligand 2	*B. taurus*
	NM_001048165	Chemokine (C–X–C motif) ligand 2	*B. taurus*
	NM_001040526	Complement factor B	*B. taurus*
	NM_174092	Interleukin 1, alpha	*B. taurus*
	NM_173923	Interleukin 6 (interferon, beta 2)	*B. taurus*
	NM_173925	Interleukin 8	*B. taurus*
	NM_174183	Selectin P	*B. taurus*
	NM_174550	Heat-shock 70 kDa protein 1A	*B. taurus*
	NM_001035293	Heat-shock 70 kDa protein 8	*B. taurus*
Regulation of apoptosis/cell death program	NM_001034735	CD74 molecule, major histocompatibility complex	*B. taurus*
	NM_001075129	Calcium channel, voltage-dependent, alpha 1A subunit	*B. taurus*
	NM_174006	Chemokine (C–C motif) ligand 2	*B. taurus*
	NM_174027	Colony stimulating factor 2 (granulocyte-macrophage)	*B. taurus*
	NM_173924	Interleukin 7	*B. taurus*
	NM_001101074	Nuclear apoptosis inducing factor 1	*B. taurus*
	NM_001075911	Nuclear receptor subfamily 4, group A, member 1	*B. taurus*
	NM_001075344	Transmembrane protein 102	*B. taurus*
	NM_173966	Tumor necrosis factor (TNF superfamily, member 2)	*B. taurus*
	NM_174092	Interleukin 1, alpha	*B. taurus*
	NM_001076409	Nuclear factor of kappa light polypeptide gene enhancer	*B. taurus*
	NM_001034536	DnaJ (Hsp40) related, subfamily B, member 13	*B. taurus*
	NM_001076031	Cell death-inducing DFFA-like effector c	*B. taurus*
	NM_173923	Interleukin 6 (interferon, beta 2)	*B. taurus*
	NM_001040490	Tumor necrosis factor receptor superfamily, member 1B	*B. taurus*
	NM_001077840	Caspase 3, apoptosis-related cysteine peptidase	*B. taurus*
	XM_604643	Caspase 7, apoptosis-related cysteine peptidase	*B. taurus*
	NM_203322	Heat shock 70 kDa protein 1A	*B. taurus*
	NM_001035419	Caspase 6, apoptosis-related cysteine peptidase	*B. taurus*
	NM_001045970	Caspase 8, apoptosis-related cysteine peptidase	*B. taurus*
	NM_001105611	CD40 molecule, TNF receptor superfamily member 5	*B. taurus*
	NM_001034676	NK2 transcription factor related, locus 3 (Drosophila)	*B. taurus*
	NM_001079645	Adenosine A3 receptor	*B. taurus*
	NM_001109796	Caspase recruitment domain family, member 11	*B. taurus*
	NM_174301	Chemokine (C–X–C motif) receptor 4	*B. taurus*
	NM_181030	Fms-related tyrosine kinase 3 ligand	*B. taurus*
	NM_174348	Intercellular adhesion molecule 1	*B. taurus*
	NM_173925	Interleukin 8	*B. taurus*
	NM_001034320	Jumonji domain containing 6	*B. taurus*
	NM_001077855	Protein kinase C, delta	*B. taurus*
	NM_001034610	Receptor-interacting serine-threonine kinase 2	*B. taurus*
	NM_001030301	Toll-like receptor adaptor molecule 1	*B. taurus*
	NM_001037100	BCL2-related protein A1	*B. taurus*
	NM_001075418	Fas apoptotic inhibitory molecule 2	*B. taurus*
	NM_001102219	NLR family, pyrin domain containing 3	*B. taurus*
	NM_001098930	Proapoptotic caspase adapter protein	*B. taurus*

Table 2. (continued)

Functional category	Gene ID	Gene name	Species
	NM_176638	Caspase 4, apoptosis-related cysteine peptidase	*B. taurus*
	NM_001034509	Caspase-15	*B. taurus*
	NM_001103097	Coagulation factor II (thrombin) receptor	*B. taurus*
	NM_001045979	Complement component 6	*B. taurus*
	NM_001035364	Complement component 9	*B. taurus*
	NM_001077963	Cytochrome c, testis	*B. taurus*
	NM_001015669	Deleted in bladder cancer 1	*B. taurus*
	NM_001102091	Engulfment and cell motility 3	*B. taurus*
	NM_001075679	Family with sequence similarity 82, member C	*B. taurus*
	NM_001040604	Growth arrest and DNA-damage-inducible, beta	*B. taurus*
	NM_001045901	Growth arrest and DNA-damage-inducible, gamma	*B. taurus*
	NM_001046113	Myocyte enhancer factor 2C	*B. taurus*
	NM_001046178	Protein phosphatase 1, regulatory (inhibitor) subunit 15A	*B. taurus*
Response to DNA damage stimuli	NM_001077840	Caspase 3, apoptosis-related cysteine peptidase	*B. taurus*
	NM_203322	Heat shock 70 kDa protein 1A	*B. taurus*

CANP1 and CANP2 in mouse myoblast C2C12 cell lines resulted in a complete prevention of migratory and myotube formation capacity of the cells. Similarly, Honda et al. (2008) found that inhibition of CANP2 blocked the fusion of myoblast C2C12 cell lines to multinucleated myotubes. Our findings report for the first time that specific knockdown of CANP1 in cattle skeletal satellite cells resulted in the reduction of viable cells in cell proliferation and finally caused the cell death.

Apoptosis or programmed cell death is orchestrated by the family of caspases including initiator caspases (e.g., caspase-8, caspase-9, and caspase-12) and effector caspases (e.g., caspase-3, caspase-6, and caspase-7) (Earnshaw et al. 1999). The genetic components of apoptosis have been reported as follows; the first involves the release of cytochrome c from mitochondria, which then binds to apoptotic protease-activating factor-1 (Apaf-1) in the apoptosome, leading to the activation of caspase-9, which then activate the effector caspases such as caspase-3, caspase-6, and caspase-7 (Grutter 2000). It was reported that the caspases cause cell death by involving the activation of caspases which in turn cleave key protein substrates; such as threonine-protein kinase (Raf-1), important for cell growth and survival (Lazebnik et al. 1995; Li et al. 1998; Luo et al. 1998; Widmann et al. 1998). In the present study, to determine whether the CANP1 knockdown reduced viable cells in cell proliferation and led to the cell death is regulated by cysteine aspartate-specific proteases (caspases), HSPs, as well as other genes, we explored the possible implication of these genes in the observed apoptotic cell death under the transfection. Our study results showed that the suppression of CANP1 led to the activation of the apoptotic caspases, also an increase in the expressions of the stress response, DNA damage-regulating genes when compared with the control. In the present study, we also found that there was a cross-talk between CANP1 and caspase system. Although, the precise mechanism of the cross-talk between CANP1 and the caspase proteolytic systems is not clearly established; however, it was hypothesized that calpain activation may be upstream or downstream of caspases (Rami 2003). We found that the suppression of CANP1 greatly increased expressions of caspases and these results implied that CANP1 activation was the downstream of caspases in our experimental model. Our study results supported the previous studies that reported a cross-talk between the calpain and the caspase systems (Del Bello et al. 2007; Liu et al. 2009). From our findings, it can be concluded that the possible mechanism by which the suppression of CANP1 led to the cell death is because of the activation of apoptotic caspases which might in turn promote the proteolysis of the proteins important for cell proliferation as well as cell survival and promote apoptosis through the caspase-dependent cell death pathway. However, further experiments are needed to elucidate the key protein substrates cleaved by these apoptotic caspases in the cell death program.

In addition to the caspase systems, the HSPs which are a family of protective proteins have been implicated in the prevention of structural damage of proteins from apoptotic processes (Beere 2005) and also the regulation of apoptosis in cells (Sreedhar and Csermely 2004). In this study, it was observed that the suppression of CANP1 resulted in an increase in HSP27, HSP70, and HSP90 expressions as assayed by RT-PCR, microarray, and Western blot. Liossis et al. (1997) reported that an over-expression of HSP70 showed enhancement of Fas-mediated apoptosis cell death in Jurkat cells while HSP90 has been reported as an important factor in helping the propagation of the apoptotic signal (Galea-Lauri et al. 1996). Also, HSP90 is necessary for the activity of the death domain

kinase and the receptor interacting protein, which sensitize cells to tumor necrosis factor-induced cell death (Lewis et al. 2000). Therefore, based on previous studies and our results, it is probably suggested that, besides the apoptotic caspase systems, HSPs are probably also involved in the apoptosis caused by CANP1 knockdown.

Conclusion

The present study found a crosstalk between CANP1 and caspase systems, in that suppression of CANP1 resulted in an activation of apoptotic caspases and HSPs expressions as well. Suppression of CANP1 resulted in a significant downregulation of proliferation, migration, and differentiation-regulating genes, suggesting that CANP1 not only plays a central role in the regulation of proliferation but also migration and differentiation of cattle skeletal satellite cells. From the results obtained in this study, it is summarized that suppression of CANP1 leads to the activation of apoptotic caspases which in turn regulate apoptosis through the caspase-dependent cell death pathway and clearly demonstrates the crucial role of CANP1 in regulation of cell proliferation as well as cell survival.

Acknowledgments It should be acknowledged that this work was supported by the research funds of Chonbuk National University in 2012, research grants for the FTA issue project (No.600 PJ907055), RDA, and the research grants for the FTA issue project (No. PJ008525), RDA, Republic of Korea.

References

Allen R. E. Muscle cell culture as a tool in animal growth research. *Fed. Proc.* 46: 290–294; 1987.

Amna T.; Shamshi Hassan M.; Ba H. V.; Khil M. S.; Lee H. K.; Hwang I. H. Electrospun Fe3O4/TiO2 hybrid nanofibers and their in vitro biocompatibility: Prospective matrix for satellite cell adhesion and cultivation. *Mater. Sci. Eng. C* 33: 707–713; 2013.

Azam M.; Andrabi S. S.; Sahr K. E.; Kamath L.; Kuliopulos A.; Chishti A. H. Disruption of the mouse u-calpain gene reveals an essential role in platelet function. *Mol. Cell. Biol.* 21: 2213–2220; 2001.

Beere H. M. Death versus survival: Functional interaction between the apoptotic and stress-inducible heat shock protein pathways. *J. Clin. Invest.* 115: 2633–2639; 2005.

Burton N. M.; Vierck J.; Krabbenhoft L.; Bryne K.; Dodson M. V. Methods for animal satellite cell culture under a variety of conditions. *Methods Cell Sci.* 22: 51–61; 2000.

Dedieu S.; Potshard S.; Mazères G.; Grise F.; Dargelos E.; Cottin P.; Brustis J. J. Myoblast migration is regulated by calpain through its involvement in cell attachment and cytoskeletal organization. *Exp. Cell Res.* 292: 187–200; 2004.

Del Bello B.; Moretti D.; Gamberucci A.; Maellaro E. Cross-talk between calpain and caspase-3/-7 in cisplatin-induced apoptosis of melanoma cells: A major role of calpain inhibition in cell death protection and p53 status. *Oncogene* 26: 2717–2726; 2007.

Dodson M. V.; Martin E. L.; Brannon M. A.; Mathison B. A.; Mcfarland D. C. Optimization of bovine satellite cell derived myotube formation in vitro. *Tissue Cell* 19: 159–166; 1987.

Earnshaw W. C.; Martins L. M.; Kaufmann S. H. Mammalian caspases: Structure, activation, substrates, and functions during apoptosis. *Annu. Rev. Biochem.* 68: 383–424; 1999.

Galea-Lauri J.; Richardson A. J.; Latchman D. S.; Katz D. R. Increased heat shock protein 90 (hsp90) expression leads to increased apoptosis in the monoblastoid cell line U937 following induction with TNF-α and cycloheximide: A possible role in immunopathology. *J. Immunol.* 157: 4109–4118; 1996.

Gandolfi G.; Pomponio L.; Ertbjerg P.; Karlsson A. H.; Costa L. N.; Lametsch R.; Russo V.; Davoli R. Investigation on CAST, CAPN1 and CAPN3 porcine gene polymorphisms and expression in relation to post-mortem calpain activity in muscle and meat quality. *Meat Sci.* 88: 694–700; 2011.

Geesink G. H.; Kuchay S.; Chishti A. H.; Koohmaraie M. Micro-calpain is essential for postmortem proteolysis of muscle proteins. *J. Anim. Sci.* 84: 834–2840; 2006.

Golding M. C.; Long C. R.; Carmell M. A.; Hannon G. J.; Westhusin M. E. Suppression of prion protein in livestock by RNA interference. *Proc. Natl. Acad. Sci. USA* 103: 5285–5290; 2006.

Goll D. E.; Thompson V. F.; Li H.; Wei W.; Cong J. The calpain system. *Physiol. Rev.* 83: 731–801; 2003.

Greenlee A. R.; Dodson M. V.; Yablonka-Reuveni Z.; Kersten C. A.; Cloud J. G. In vitro differentiation of myoblasts from skeletal muscle of rainbow trout *Oncorhynchus mykiss*. *J. Fish Biol.* 46: 731–747; 1995.

Grutter M. G. Caspases: Key players in programmed cell death. *Curr. Opin. Struct. Biol.* 10: 649–655; 2000.

Honda M.; Masui F.; Kanzawa N.; Tsuchiya T.; Toyo-oka T. Specific knockdown of m-calpain blocks myogenesis with cDNA deduced from the corresponding RNAi. *Am. J. Physiol. Cell Physiol.* 294: C957–C965; 2008.

Huang Y.; Wang K. K. W. The calpain family and human disease. *Trend. Mol. Med.* 7: 355–362; 2001.

Huff-Lonergan E.; Lonergan S. M. Mechanisms of water-holding capacity of meat: The role of postmortem biochemical and structural changes. *Meat Sci.* 71: 194–204; 2005.

Huttenlocher A.; Palecek S. P.; Lu Q.; Zhang W.; Mellgren R. L.; Lauffenburger D. A.; Ginsberg M. H.; Horowitz A. F. Regulation of cell migration by the calcium-dependent protease calpain. *J. Biol. Chem.* 272: 32719–32722; 1997.

Jain H.; Singh H.; Kadam M.; Sarkhel B. C. Knockdown of the myostatin gene by RNA interference in caprine fibroblast cells. *J. Biotechnol.* 145: 99–102; 2010.

Kemp C. M.; Sensky P. L.; Bardsley R. G.; Buttery P. J.; Parr T. Tenderness—An enzymatic view. *Meat Sci.* 84: 248–256; 2010.

Kent M. P.; Spencer M. J.; Koohmaraie M. Postmortem proteolysis is reduced in transgenic mice overexpressing calpastatin. *J. Anim. Sci.* 82: 794–801; 2004.

Koohmaraie M.; Seideman S. C.; Schollmeyer J. E.; Dutson T. R.; Crouse J. D. Effects of post-mortem storage on Ca^{2+}-dependent proteases, their inhibitor and myofibril fragmentation. *Meat Sci.* 19: 187–196; 1987.

Lazebnik Y. A.; Takahashi A.; Moir R. D.; Goldman R. D.; Poirier G. G.; Kaufmann S. H.; Earnshaw W. C. Studies of the lamin proteinase reveal multiple parallel biochemical pathways during apoptotic execution. *Proc. Natl. Acad. Sci. USA* 92: 9042–9046; 1995.

Lewis J.; Devin A.; Miller A.; Lin Y.; Rodriguez Y.; Neckers L.; Liu Z. G. Disruption of hsp90 function results in degradation of the death domain kinase, receptor-interacting protein (RIP), and blockage of

tumor necrosis factor-induced nuclear factor-kappa B activation. *J. Biol. Chem.* 275: 10519–10526; 2000.

Li H.; Zhu H.; Xu C.; Yuan J. Cleavage of BID by caspase 8 mediates the mitochondrial damage in the Fas pathway of apoptosis. *Cell* 94: 491–501; 1998.

Liossis S. N.; Ding X. Z.; Kiang J. G.; Tsokos G. C. Overexpression of the heat shock protein 70 enhances the TCR/CD3-and Fas/Apo-1/CD95-mediated apoptotic cell death in Jurkat T cells. *J. Immunol.* 158: 5668–5675; 1997.

Liu L.; Xing D.; Chen W. R. μ-Calpain regulates caspase-dependent and apoptosis inducing factor-mediated caspase-independent apoptotic pathways in cisplatin-induced apoptosis. *Int. J. Cancer* 125: 2757–2766; 2009.

Luo X.; Budihardjo I.; Zou H.; Slaughter C.; Wang X. Bid, a Bcl2 interacting protein, mediates cytochrome C release from mitochondria in response to activation of cell surface death receptors. *Cell* 94: 481–490; 1998.

Pfaffl M. W. A new mathematical model for relative quantification in real-time PCR. *Nucleic Acids Res*. 29: e45; 2001.

Potter D. A.; Tirnauer J. S.; Janssen R.; Croall D. E.; Hughes C. N.; Fiacco K. A.; Mier J. W.; Maki M.; Herman I. M. Calpain regulates actin remodeling during cell spreading. *J. Cell Biol.* 141: 647–662; 1998.

Rami A. Ischemic neuronal death in the rat hippocampus: The calpain calpastatin-caspase hypothesis. *Neurobiol. Dis.* 13: 75–88; 2003.

Reynolds A.; Leake D.; Boese Q.; Scaringe S.; Marshall W. S.; Khvorova A. Rational siRNA design for RNA interference. *Nat. Biotechnol.* 22: 326–330; 2004.

Rhoads R. P.; Fernyhough M. E.; Liu X.; McFarland D. C.; Velleman S. G.; Hausman G. J. Extrinsic regulation of domestic animal-derived myogenic satellite cells II. *Domest. Anim. Endocrinol.* 36: 111–126; 2009.

Sorimachi H.; Ishiura S.; Suzuki K. Structure and physiological function of calpains. *Biochem. J.* 328: 721–732; 1997.

Sreedhar A. S.; Csermely P. Heat shock proteins in the regulation of apoptosis: new strategies in tumor therapy: A comprehensive review. *Pharmacol. Ther.* 101: 227–257; 2004.

Widmann C.; Gibson S.; Johnson G. L. Caspase-dependent cleavage of signaling proteins during apoptosis. A turn-off mechanism for anti-apoptoticnsignals. *J. Biol. Chem.* 273: 7141–7147; 1998.

Xia H.; Mao Q.; Paulson H. L.; Davidson B. L. siRNA-mediated gene silencing in vitro and in vivo. *Nat. Biotechnol.* 20: 1006–1010; 2002.